

Insights on the Facet Specific Adsorption of Amino Acids and Peptides toward Platinum

Sathish Kumar Ramakrishnan,^{†,§} Marta Martin,^{†,§} Thierry Cloitre,^{†,§} Lucyna Firlej,^{†,§} Frédéric J. G. Cuisinier,[‡] and Csilla Gergely^{*,†,§}

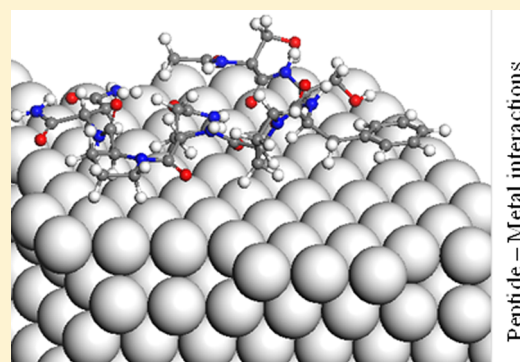
[†]Université Montpellier 2, Laboratoire Charles Coulomb UMR 5221, F-34095, Montpellier, France

[§]CNRS, Laboratoire Charles Coulomb UMR 5221, F-34095, Montpellier, France

[‡]UFR Odontologie, EA4203, Université Montpellier 1, Montpellier, 34193, France

Supporting Information

ABSTRACT: Engineering shape-controlled bionanomaterials requires comprehensive understanding of interactions between biomolecules and inorganic surfaces. We explore the origin of facet-selective binding of peptides adsorbed onto Pt(100) and Pt(111) crystallographic planes. Using molecular dynamics simulations, we show that upon adsorption the peptides adopt a predictable conformation. We compute the binding energies of the amino acids constituting two adhesion peptides for Pt, S7, and T7 and demonstrate that peptides' surface recognition behavior that makes them unique among populations originates from differential adsorption of their building blocks. We find that the degree of peptide binding is mainly due to polar amino acids and the molecular architecture of the peptides close to the Pt facets. Our analysis is a first step in the prediction of enhanced affinity between inorganic materials and a peptides, toward the synthesis of novel nanomaterials with programmable shape, structure, and properties.



INTRODUCTION

Physico-chemical properties of nanomaterials rely on their shape. Therefore, an adequate design and shape-controlled synthesis of nanocrystals can pave the way to engineer materials with properties fitting *a priori* any desired applications. To be efficient, this process requires full control and predictability of the resulting structures.¹ An increasing interest in fabricating complex nanomaterials with the help of biomolecules starts to emerge.^{2,3} The implementation of phage display combinatorial technology into material science has revolutionized the biomimetic engineering of materials by selecting a highly competitive polypeptide binder among a population of billions.^{4–6} Enhanced binding sensitivity of 12-mer peptides against various inorganic surfaces via a biomimetic molecular evolutionary approach was reported.^{7,8} The peptides constitute an alternative to grafting chemistry and might serve as bifunctional specific linkers, assuring a controlled recognition between the surface and biomolecules at an atomic level.⁹ Usually, the distribution of particles on a surface is described by a random sequential adsorption model with an adsorption probability equal to $\exp[-U(r)/kT]$, where $U(r)$ is the potential acting between the free particle and the particles already deposited on the surface.¹⁰ Peptide interaction with the surface has a more complex nature and involves polar binding, hydrogen bonding, electrostatic, and van der Waals forces. Control of these interactions is necessary to design hybrid molecular structures with various potential applications.

Understanding the mechanism that makes peptides recognize the target molecules or surfaces is essential for programmable, biomimetic material synthesis. Today, the knowledge of the nature of molecular interactions underlying this process is still sparse.^{11–14} Recently, a successful, biomimetically regulated growth of gold and silver nanoparticles was reported.^{15,16} Among noble metals, platinum (Pt) has also been extensively studied for its excellent catalytic activity that is strongly dependent on the different crystallographic facets of the material.¹⁷ Size and shape selective synthesis of platinum nanocrystals using peptides was also achieved.^{18,19} Phage display technology allowed us previously to select two adhesion peptides S7 (Ac-Ser-Ser-Phe-Pro-Gln-Pro-Asn-CONH₂) and T7 (Ac-Thr-Leu-Thr-Thr-Leu-Thr-Asn-CONH₂) (Figure 1) to study the selective recognition of Pt(111) and Pt(100) crystallographic facets.²⁰ The authors

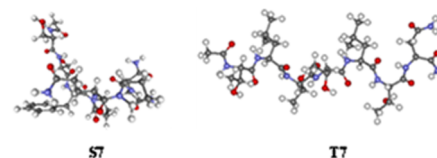


Figure 1. Models of peptide S7 and T7.

Received: October 29, 2013

Published: December 2, 2013

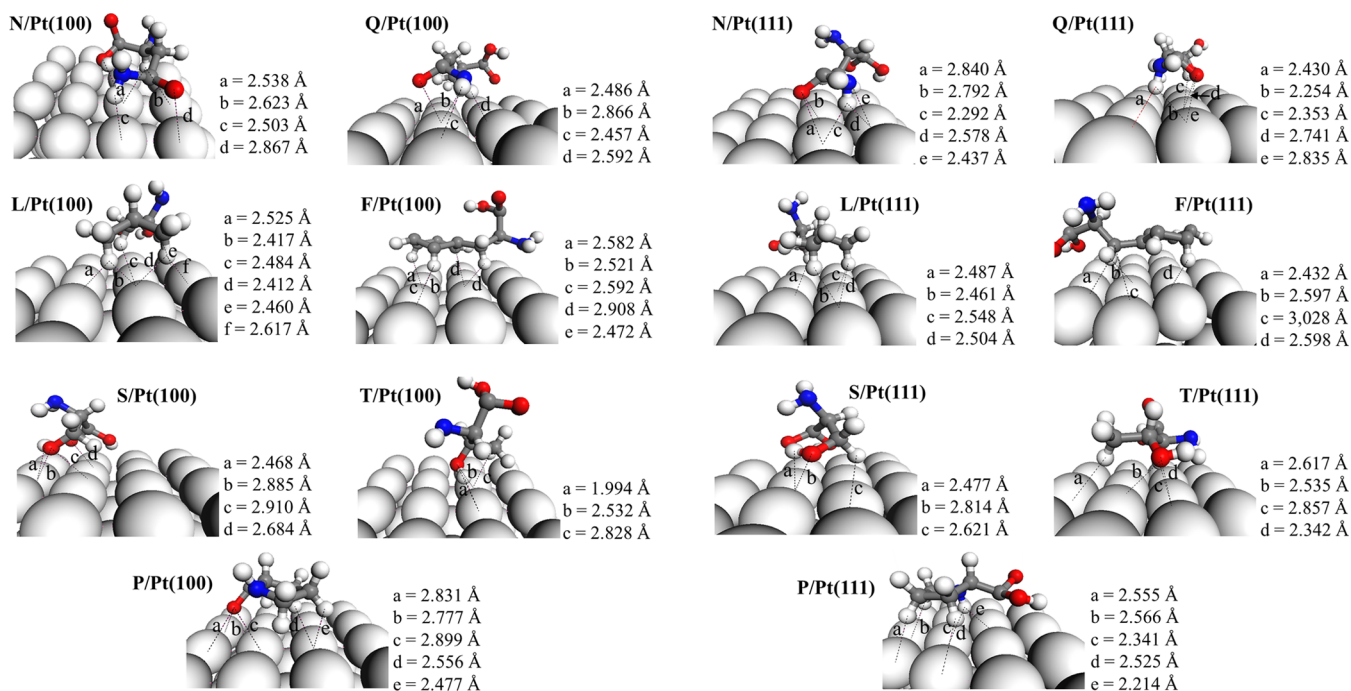


Figure 2. Optimized configuration of amino acids adsorbed on Pt(100) and Pt(111) surface. Dotted lines indicate distances between amino acids and the surface, as discussed in the text (atoms located at less than 3 Å).

pointed out the possibility of peptide-regulated synthesis of Pt nanocrystals, as the presence of peptides facilitates the growth of specific crystallographic orientations. In fact, the Pt(100)-specific T7 binding peptide favored the growth of cubic nanocrystals, whereas the Pt(111) binding S7 peptide produced tetrahedrons.²⁰ Transformation from one shape to the other was possible by switching the type of adhesion peptide in the solution, a process certainly induced by the interaction between the binding peptides and the Pt surface atoms. Though the knowledge on the recognition process between inorganic surfaces and peptides is still limited, it is admitted that interaction between peptides and the surface occurs via amino acid side chains. Therefore, to finely tune the biomolecule specificity toward a material, it is essential to gain insight into the mechanism of substrate recognition at the amino acid level. Molecular dynamics simulations were used in the past to address the influence of surface shape on adsorption of peptides toward gold surface.¹⁹ Here, we present a detailed computational study of the molecular recognition of platinum Pt(111) and Pt(100) surfaces by selected amino acids that we further extend to the analysis of peptide adsorption mechanisms.

■ COMPUTATIONAL DETAILS

Atomistic Models of Amino Acids, Peptides, and Platinum Crystalline Facets. Atomistic models of amino acids, peptides, and Pt crystalline facets were prepared in Argus Lab and Materials Studio (MS) visualizer. The zwitterionic configuration of amino acids and peptides were considered in aqueous solution at pH = 7. Pt(100) and Pt(111) surfaces were prepared using standard lattice parameters. Geometry optimization of Pt surface was carried out using density functional theory (DFT) code implemented in the MS CASTEP module.²¹ Perdew-Burke-Ernzerhof (PBE) – Generalized Gradient Approximation (GGA) functional was employed to account for the exchange correlation effects. The energy cut off was set at 310 eV. The self-consistent field (SCF) convergence

parameters were set at 1×10^{-5} eV and the maximum stress component at 0.05 GPA. After geometry optimization, the surface was cleaved according to Miller indices to a thickness of 5 atomic layers to form Pt(100) and Pt(111) surfaces. The energy of amino acids and peptides was minimized in vacuum using the conformational analysis tool of HyperChem molecular modeling system. This method allowed us to generate the low energy conformations by varying dihedral angles while high energy structures were discarded.²² Out of several hundred generated structures, for further molecular dynamics simulations we have selected the low energy conformations as global minimum structure. The resulting low energy structures of amino acids and peptides were solvated with explicit water and minimized for 500 steps via the conjugate gradient (Polak – Ribiere algorithm) method with the convergence of 0.1 kJ/mol using CHARMM 27 force field.²³

Simulation Protocol for Adsorption of Amino Acids and Peptides. Molecular dynamics (MD) simulations were employed to study the adsorption of seven facet specific amino acids [Gln(Q), Phe(F), Asn(N), Leu(L), Thr(T), Ser(S), and Pro(P)] constituting the adhesion peptides (S7 and T7) for Pt(100) and Pt(111) surfaces. All simulations were performed using the MS Discover program²¹ with constant valence force field (CVFF) parameters.²⁴ The dimensions of simulation cells were typically 1.1 nm × 1.1 nm × z. The height z of the cell is system dependent and equals 0.92 nm for metal, 2.9 nm for the metal–amino acid, and 4.4 nm for the metal–amino acid–solvent systems. All atoms of the Pt crystallographic facets are fixed during the simulations. 200 water molecules were used for amino acid solvation calculations and more than 800 molecules for peptide systems. The potential energy does not vary after five layers of Pt;²² therefore, the five atomic layers of Pt were considered as an optimal crystallographic thickness of the substrate. To evaluate the amino acids side chains' specificity toward (100) and (111) platinum surfaces, the optimized

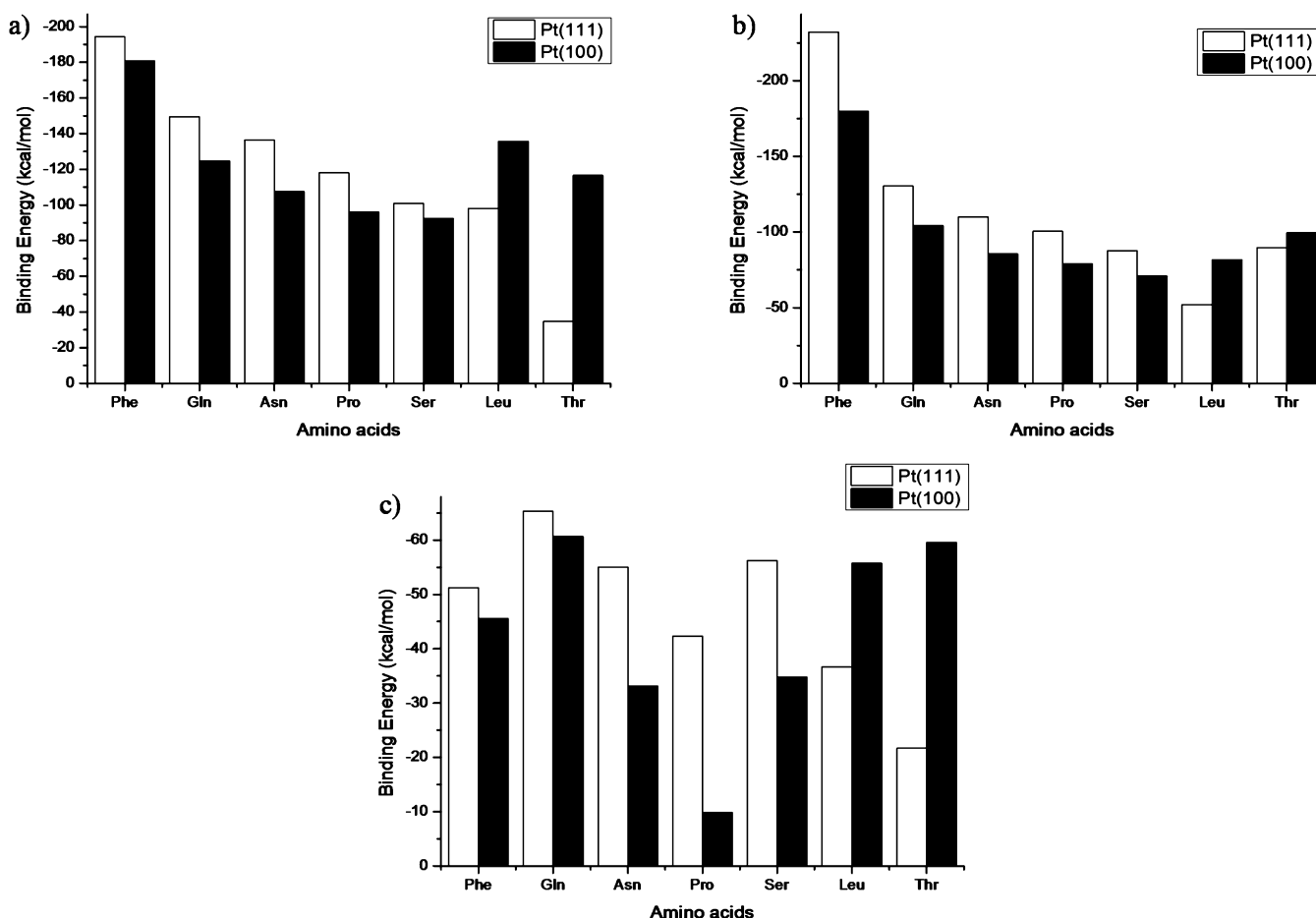


Figure 3. Adsorption energies (kcal/mol) of amino acids toward platinum crystalline facets in (a) ionic solution, (b) water, and (c) vacuum.

geometries of facet specific amino acids were placed on the crystalline Pt surfaces and MD simulations were carried out in (a) vacuum, (b) water, and (c) ionic solution (130 mM phosphate buffer, PBS, pH 7). To equilibrate the system, we first performed system energy minimization for 2 ns, then the production runs were carried out in NVT ensemble ($T = 300$ K, $p = 1$ atm) for 30–40 ns in vacuum and 80–100 ns in liquid environment, respectively.

All possible peptide-Pt facet combinations have been explored: S7–Pt(111), S7–Pt(100), T7–Pt(100), and T7–Pt(111). Box dimensions for the peptide–metal system were $2.2 \text{ nm} \times 2.2 \text{ nm} \times z$, where z is the box height: 1.2 nm for metal and 3.9 nm for the metal–peptide system, respectively. Peptide adsorption was considered in the presence of water (>700 molecules, TIP3P model) and buffering ions (130 mM). The Pt-peptide systems were first equilibrated for 5 ns; the production runs (molecular dynamics in NVT ensemble with 1.0 fs time step) lasted for 100 ns. Molecular trajectories were recorded every 1 ns for analysis to reveal the peptide molecule behavior toward the surface. We set the temperature to 300 K (Andersen thermostat) and the coulombic interactions at about 0.01 kcal/mol.

RESULTS AND DISCUSSION

In the first step of our work, we simulated (MD) the adsorption on platinum of seven facet-specific amino acids that constitute S7 and T7 peptides on Pt(100) and Pt(111) facets. Though these peptides have been selected by combinatorial phase

Table 1

amino acids	E_a (kcal/mol)					
	Pt(111) Solution	Pt(100) Solution	Pt(111) Water	Pt(100) Water	Pt(111) Vacuum	Pt(100) Vacuum
Phe	−194	−181	−232	−180	−51	−46
Gln	−149	−125	−130	−104	−65	−61
Asn	−136	−108	−110	−86	−55	−33
Pro	−118	−96	−100	−79	−42	−10
Ser	−101	−93	−88	−71	−56	−35
Leu	−98	−136	−52	−82	−37	−56
Thr	−35	−117	−90	−99	−22	−60

Table 2. Peptide–Substrate Adsorption Energies (kcal/mol) of S7 and T7 on Different Pt Facets

peptides	platinum facets	
	Pt (100) (kcal/mol)	Pt (111) (kcal/mol)
S7	−55	−148
T7	−145	−88

display as the ones with highest affinity toward Pt, the influence of individual amino acid on peptide adsorption remained unclear. Figure 2 shows the optimized structures of amino acids adsorbed on Pt (100) and Pt (111), provided by our simulations. The dotted lines indicate the calculated shortest distances between the adsorbed amino acids and the surface.

The sequences of the S7 (Ac–Ser–Ser–Phe–Pro–Gln–Pro–Asn–CONH₂) and T7 (Ac–Thr–Leu–Thr–Thr–Leu–

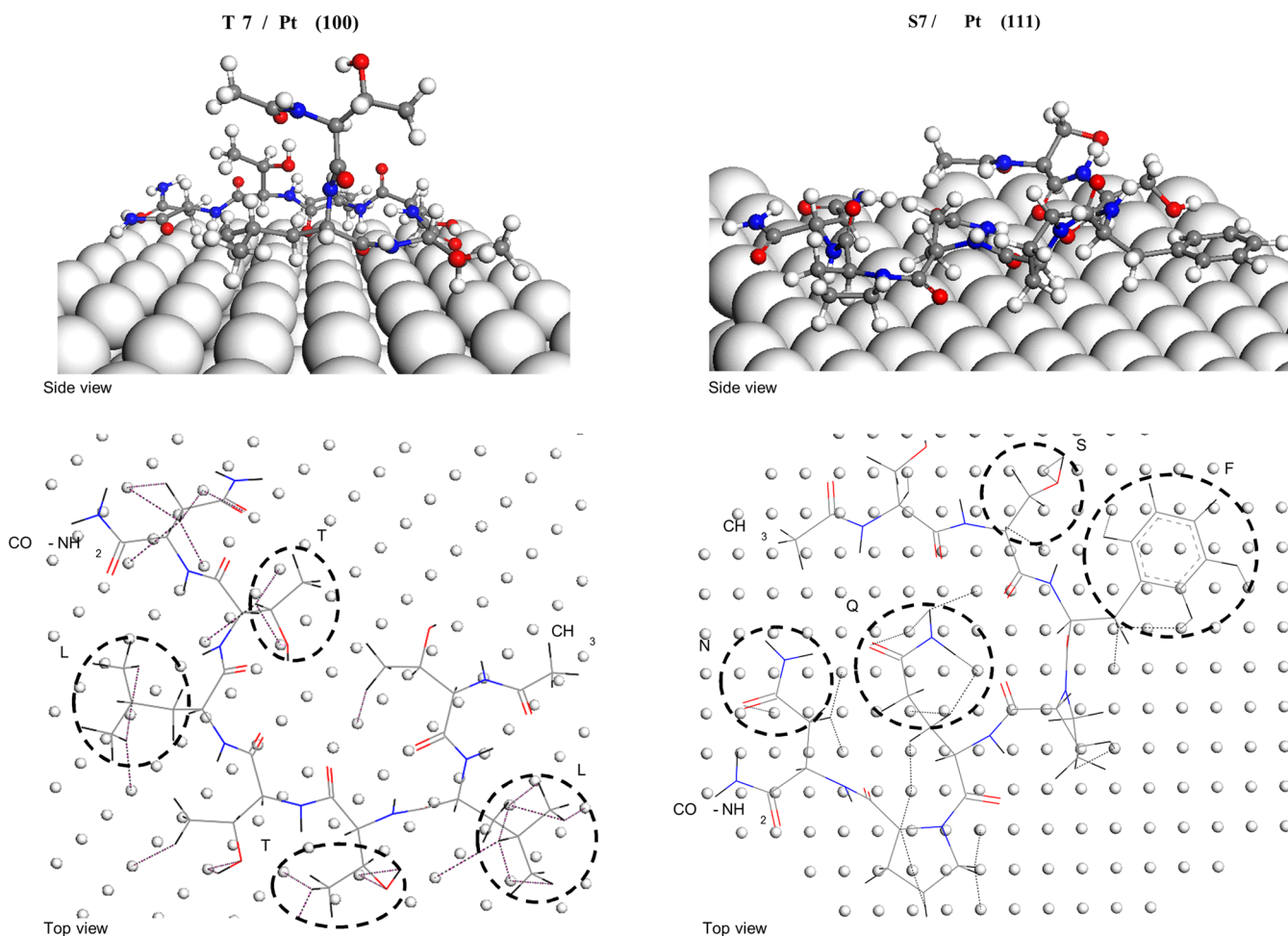


Figure 4. Surface specificity prediction: top view and side view of S7 and T7 peptide on Pt(100) and Pt(111) surface. Configurations of T, L and N, Q, S and F amino-acids, yielding to the strongest peptide interactions with Pt(100) and Pt(111), respectively are indicated by dotted circles. Water molecules were omitted for visual clarity.

Thr–Asn–CONH₂) peptides are different: the only common amino acid is the Asn. They do not contain charged amino acids, only polar uncharged and nonpolar hydrophobic. To investigate the role of hydrophobic and ionic interactions, simulation on amino acid adsorption has been carried out in three different environments: in aqueous, in ionic solution, and in vacuum. The adsorption energies of each amino acid were calculated using the standard interaction energy equation:

$$E_{\text{Ads}} = E_{\text{S-AA}} - (E_{\text{S}} + E_{\text{AA}}) \quad (1)$$

where E_{S} is the energy of the Pt surface, E_{AA} is the energy of the amino acid, and $E_{\text{S-AA}}$ is the energy of the system (surface + amino acids). The adsorption energies of the solvated amino acids were calculated using the following equation:¹¹

$$E_{\text{Ads}} = E_1 - E_2 + E_3 - E_4 \quad (2)$$

where E_1 , E_2 , E_3 , and E_4 are the average energies of the surface–amino acid–solvent system, the amino acid–solvent system, the solvent system, and the surface–solvent system, respectively.

The calculated energies of amino acid adsorption on Pt(100) and Pt(111)²⁴ are shown in Figure 3. The average distances between the amino acids (in vacuum) and the Pt surface are summarized in Table S1 of Supporting Information. The results are consistent with previous theoretical simulations²² and

experimental observations.²⁵ This validates our choice of the force field used to describe interactions in the systems studied. The adsorption energy primarily depends on the size, conformation, polarity and charge of the amino acid, the crystal morphology, and the contact area between the amino acid and surface. The strength of binding defines the distance between the side chain atoms of amino acids and the metal surface. Generally, we consider that a direct contact occurs when this distance is less than 3 Å.

Table 1 gives the adsorption energies calculated in vacuum, water, and ionic solution. The energies are higher when amino acids are in aqueous solution. It indicates that the presence of water and ions is crucial in mediating the peptide adsorption process; evaluating amino acid adsorption in vacuum gives only a crude idea about the mechanism of amino acid binding to the substrate.

In fact, specificity of interactions between amino acids and surface depends not only on the structure of amino acids and surface morphology, but also on the presence of interfacial water layer. Solvated conditions in simulations better mimic a realistic experimental adsorption environment. Recently, it was demonstrated that water prefers binding at atop sites and lies parallel to the surface.²⁶ In this case an additional transient state barrier appears due to the presence of a hydration layer

preventing the direct contact between amino acids and the surface.

The Na^+ , K^+ , and Cl^- ions in the PBS buffer are the early members of the Hofmeister series. They strengthen the hydrophobic interactions by salting out in amino acids. This can be seen in the increased binding energy values of the Pro and Leu hydrophobic amino acids as well as in the case of Phe adsorption onto Pt (100), relative to those obtained in water (Figure 3, or Table 1). The presence of ions slightly changes the binding of amino acids to Pt surfaces. It is mainly due to screening of electrostatic interactions by ions. It has been also reported that, as Na^+ and K^+ ions adsorb directly onto the metal surface (contrary to later members of the Hofmeister series),²⁷ their presence reduces only slightly the translation motion of water.²⁸ We have not observed during the simulation any significant loss of the degrees of freedom for water bound peptides, but a small conformational entropic loss upon adsorption on water and surface.²⁸ It has been demonstrated that the conformational entropy of the peptides upon adsorption can either decrease or increase.²⁹ Computation of entropy and free energy is more time-consuming than that of energies, because very well resolved histograms of energy distribution are needed or multiple simulations for each system.¹¹ An evaluation of loss in entropic freedom for a 12-peptide can be made by taking into account the rotatable bounds of the peptide; it leads to a value of $-T\Delta S \approx 48 \text{ kT}$.⁹ Concomitantly, this loss can be partially compensated by an entropic gain due to release of water molecules.¹¹ Our calculations also show that whatever the environment, Phe, Gln, Asn, and Pro bind more strongly to the Pt(111) surface, whereas Leu and Thr prefer the Pt(100) facet. Upon closer examination it turns out that phenylalanine (Phe, P), the most hydrophobic aromatic amino acid, displays the highest affinity to both surfaces though the adsorption energy is higher toward the Pt(111) facet. Phe was already suggested to be a key factor in enhancing peptide specificity toward Pt(111).³⁰ It has been demonstrated³¹ that the hydrogen atoms closest to the Pt surface lean out of the Phe benzene ring by 7.3° yielding to the formation of Pt–C bonds. Thus, benzene C atoms exhibit partial sp^3 hybridization in contrast to the original sp^2 hybridization.

Glutamine (Gln, Q), a highly polar amino acid shows the second highest adsorption energy on Pt, in agreement with previous results.²⁵ Because of Gln's hydrophilic nature the distance between the amino acid side chains and the Pt surface is short, with a contact at an average distance of 2.6 Å. Asparagine (Asn, N), another polar amino acid, binds strongly to both Pt(111) and (100) facets. Both Gln and Asn act as electron donor/acceptors, which might facilitate their binding toward platinum. Serine (Ser, S), a polar amino acid comporting a hydroxyl group binds also to both Pt surfaces, similarly to Asn. In general, the binding energies of polar amino acids (Gln, Asn, Ser) relative to the hydrophobic Phe is lower in solution than in vacuum.

Among the amino acid studied in this work, Proline (Pro, P) adsorbs the least onto the Pt(100) facet in vacuum and presents higher affinity for the Pt(111) than for the Pt(100) facet in solution. Proline, generally found in weak binders, is unique among the naturally occurring amino acids; its side chain wraps around to form a covalent bond with the backbone, severely restricting the backbone conformation of neighboring residues.³² The presence of Pro in a peptide confers a higher structural constraint to the peptide that could facilitate Pro

adhesion onto the surface. We found that, when adsorbed on Pt(111), Pro side chains are located near the surface (at 2.44 Å), eventually enabling the formation of hydrogen bonds with the Pt surface. The observed difference in Pro affinity toward the two Pt crystallographic facets may arise from the variations in surface morphology of the two substrates.

Leucine (Leu, L) and Threonine (Thr, T), comporting methyl and hydroxyl groups, play a key role in adsorption on Pt(100) surface. Their average distance from the substrate, 2.486 and 2.451 Å, respectively, are lower than for the Pt(111) surface. The mechanism of adsorption consists of first a detachment of hydrogen ion from the methyl group, followed by the attachment of a charged carbon to Pt.³³ It is interesting to note that, among the amino acids, Leu and Thr show the lowest affinity toward the (111) facet.

On the contrary, the presence of N atoms and amine (NH_2) groups in Gln, Asn, and Pro seems to enhance amino acid affinity toward the Pt(111) facet. This result agrees with previous suggestions that both amine and hydroxyl groups (in Ser in our case) increase binding, especially on (111) metal surfaces.^{20,22} Besides the specific configuration of amino acid side chains, differential adsorption could arise from the way their conformation matches the morphology of the substrate crystalline facets.

To summarize, our calculations indicate that the best binders for the Pt(111) surface are the Phe, Gln, Asn, Ser, and Pro, whereas Phe, Gln, Asn, Ser, Leu, and Thr are good linkers for the Pt(100) surface. Taking into account the differences in binding energies of Phe, Gln, Asn, and Ser on both Pt facets, we conclude that the best candidates for facet Pt(111) specific crystal growth are Phe, Gln, Pro, and Asn, whereas Leu and Thr behave as specific Pt(100) facet binders. However, it is clear that, rather than individual amino acids, there is a combination of a few specific amino acid sides in a chain that defines peptide-specific crystal growth. Therefore, we extended our study to S7 and T7 peptide adsorption on both Pt crystalline facets, using molecular dynamics simulation and calculated (eq 2) the adsorption energies of peptides by replacing amino acid system values with peptides values.

Generally, the peptide adhesion strongly depends on the initial peptide orientation with respect to the surface. To avoid an artificial quenching of the structure in a metastable configuration during MD simulations, 12 different peptide configurations were prepared by consecutive 30° rotations, covering a whole turn of the structure, placed on different Pt crystallographic facets, and allowed to adsorb and stabilize. The configuration presenting the highest adsorption energy has then been selected as the optimal structure of the adsorbed peptide.

Calculated peptide-surface adsorption energies are gathered in Table 2. The values are in the range of those obtained for individual amino acids in a liquid environment. Peptide S7 displays 3-fold higher affinity toward Pt(111) than toward Pt(100). The affinity of peptide T7 toward Pt(111) is nearly 2-fold higher than that toward Pt(100). The optimal S7 and T7 conformations on Pt(111) and Pt(100) facets are shown in Figure 4. Both peptides realize multiple contacts with the surface. Upon close inspection, Phe and Gln (Figure 4 encircled) are the most important contributors to S7–Pt(111) affinity as their adsorption distances are less than 3 Å. This is in very good agreement with our previous observation of preferential attachment of these amino acids onto the Pt(111) facet. We conclude that the adsorption behavior of the S7 peptide is similar to that of its building

blocks. Similarly, in T7 peptide, where Thr and Leu are in juxtaposition within the peptide chain, they are the best binders for the Pt(100) facet. The detailed analysis of the molecular recognition process of T-L pairs and their affinity toward Pt(100) will be the subject of future work. The snapshots of representative MD conformations of peptides before and after adsorption on Pt are presented in SI-1 (SI = Supporting Information) for T7–Pt(100), T7–Pt(111), S7–Pt(111), and S7–Pt(100). Substantial conformation changes upon adsorption were observed, in each peptide and for both Pt facets (see SI-1 and SI-2). A detailed list of amino acid contact points in the S7 and T7 peptides, including adsorption distances, are given in SI-3.

The accuracy of our calculations obviously depends on the quality of the force field parameters (we used CVFF²⁴) and limitations of computational time (to test several configurations to obtain the quantitative description of the peptide adsorption). Although we consider that the relative properties and structures of amino acids adsorbed on Pt are correctly reproduced with CVFF parameters, the absolute values of the adsorption energies must be checked using different force fields, elaborated specifically to simulate the phenomena occurring at metal interfaces.³⁴ Ruang et al. have recently reported that, when using CHARMM-METAL force field, lower binding energies between the S7 peptide and the Pt(111) are obtained.³⁰ To evaluate the effect of other force fields we have performed the calculations with both standard CVFF²⁴ and improved CVFF³⁴ force fields. We found that the standard CVFF overestimated the binding energy of amino acids in solution (Figure SI4). However, this difference in absolute energy values do not modify the major adsorption trend of amino acids and does not influence the peptide surface recognition properties, namely, that S7 prefers Pt(111), while T7 prefers the other Pt(100) facet, respectively. Compared to previous works, when a key role for Phe in enhancing peptide specificity toward Pt(111) has been already suggested³⁰ we report here on the contribution of other amino acid too in peptide binding against both Pt(111) and Pt(100) facets. Also, our calculations providing the configuration of the T7 peptide on Pt(100) reveal the role of T-L pairs in the adsorption process.

CONCLUSIONS

We demonstrate that peptide adsorption on a Pt surface can be partially interpreted in terms of the interaction between metal surface and peptide building blocks. We identify the best binding amino acids for the Pt(100) and Pt(111) surfaces and show that some of them preferentially adsorb on one of the Pt crystalline facets. These differences may originate from surface morphology and the presence of reactive amino acid groups (polar and amine). However, most of amino acids bind to both surfaces with comparable strength. It suggests that the experimentally observed differential facet affinity of the S7 and T7 peptides cannot be explained by peptide composition (in terms of their building blocks) only. The sequence of amino acids, and the resulting peptide flexibility and mobility, must be considered, too.

More importantly, our study demonstrates that upon adsorption binding peptides align in a predictable geometry on Pt crystallographic surfaces. Such a clear picture of the strongly bound and free parts of the peptide is invaluable when further peptide modifications are proposed (for example with capture agents) in sensing applications. Combining MD

simulations of amino acid trajectories toward Pt and the computed molecular structure of the adsorbed peptides provides a good insight on their surface recognition mechanisms, paving the way to engineering peptide sequences with enhanced affinity to a given surface.

ASSOCIATED CONTENT

Supporting Information

Molecular dynamics simulation results including table and Figures SI1–SI4. This material is available free of charge via the Internet at <http://pubs.acs.org>.

AUTHOR INFORMATION

Corresponding Author

*E-mail: Csilla.gergely@univ-montp2.fr.

Author Contributions

The manuscript was written through contributions of all authors. All authors have given approval to the final version of the manuscript.

Notes

The authors declare no competing financial interest.

ACKNOWLEDGMENTS

We are thankful for the support of computational resources provided by Centre Informatique National de l'Enseignement Supérieur (CINES). We thank Atilla Vegh for his support.

REFERENCES

- (1) Xia, Y.; Xiong, Y.; Lim, B.; Skrabalak, S. E. Shape-controlled synthesis of metal nanocrystals: simple chemistry meets complex physics? *Angew. Chem., Int. Ed. Engl.* **2009**, *48* (1), 60–103.
- (2) Mao, C. B.; Solis, D. J.; Reiss, B. D.; Kottmann, S. T.; Sweeney, R. Y.; Hayhurst, A.; Georgiou, G.; Iverson, B.; Belcher, A. M. Virus-based toolkit for the directed synthesis of magnetic and semiconducting nanowires. *Science* **2004**, *303* (5655), 213–217.
- (3) Nam, K. T.; Kim, D. W.; Yoo, P. J.; Chiang, C. Y.; Meethong, N.; Hammond, P. T.; Chiang, Y. M.; Belcher, A. M. Virus-enabled synthesis and assembly of nanowires for lithium ion battery electrodes. *Science* **2006**, *312* (5775), 885–888.
- (4) Feldheim, D. L.; Eaton, B. E. Selection of biomolecules capable of mediating the formation of nanocrystals. *ACS Nano* **2007**, *1* (3), 154–9.
- (5) Whaley, S. R.; English, D. S.; Hu, E. L.; Barbara, P. F.; Belcher, A. M. Selection of peptides with semiconductor binding specificity for directed nanocrystal assembly. *Nature* **2000**, *405* (6787), 665–668.
- (6) Brown, S. Metal-recognition by repeating polypeptides. *Nat. Biotechnol.* **1997**, *15* (3), 269–272.
- (7) Estephan, E.; Saab, M.-B.; Agarwal, V.; Cuisinier, F. J. G.; Larroque, C.; Gergely, C. Peptides for the biofunctionalization of silicon for use in optical sensing with porous silicon microcavities. *Adv. Funct. Mater.* **2011**, *21* (11), 2003–2011.
- (8) Estephan, E.; Larroque, C.; Bec, N.; Martineau, P.; Cuisinier, F. J.; Cloitre, T.; Gergely, C. Selection and mass spectrometry characterization of peptides targeting semiconductor surfaces. *Biotechnol. Bioeng.* **2009**, *104* (6), 1121–31.
- (9) Tsurkan, M. V.; Chwalek, K.; Levental, K. R.; Freudenberg, U.; Werner, C. Modular StarPEG-heparin gels with bifunctional peptide linkers. *Macromol. Rapid Commun.* **2010**, *31* (17), 1529–1533.
- (10) Senger, B.; Schaaf, P.; Bafaluy, F. J.; Cuisinier, F. J. G.; Talbot, J.; Voegel, J. C. Adhesion of hard-spheres under the influence of double-layer, van-der-Waals, and gravitational potentials at a solid-liquid interface. *Proc. Natl. Acad. Sci., U.S.A.* **1994**, *91* (8), 3004–3008.
- (11) Heinz, H.; Farmer, B. L.; Pandey, R. B.; Slocik, J. M.; Patnaik, S. S.; Pachter, R.; Naik, R. R. Nature of molecular interactions of peptides

with gold, palladium, and Pd-Au bimetal surfaces in aqueous solution. *J. Am. Chem. Soc.* **2009**, *131* (28), 9704–9714.

(12) Verde, A. V.; Acres, J. M.; Maranas, J. K. Investigating the specificity of peptide adsorption on gold using molecular dynamics simulations. *Biomacromolecules* **2009**, *10* (8), 2118–2128.

(13) Monti, S.; Carravetta, V.; Battocchio, C.; Iucci, G.; Polzonetti, G. Peptide/TiO₂ surface interaction: A theoretical and experimental study on the structure of adsorbed ALA-GLU and ALA-LYS. *Langmuir* **2008**, *24* (7), 3205–3214.

(14) Di Felice, R.; Corni, S. Simulation of peptide–surface recognition. *J. Phys. Chem. Lett.* **2011**, *2* (13), 1510–1519.

(15) Brown, S.; Sarikaya, M.; Johnson, E. A genetic analysis of crystal growth. *J. Mol. Biol.* **2000**, *299* (3), 725–735.

(16) Naik, R. R.; Stringer, S. J.; Agarwal, G.; Jones, S. E.; Stone, M. O. Biomimetic synthesis and patterning of silver nanoparticles. *Nat. Mater.* **2002**, *1* (3), 169–172.

(17) Somorjai, G. A.; Li, Y. *Introduction to surface chemistry and catalysis*; Wiley-VCH, 1994.

(18) Yin, A.-X.; Min, X.-Q.; Zhang, Y.-W.; Yan, C.-H. Shape-selective synthesis and facet-dependent enhanced electrocatalytic activity and durability of monodisperse sub-10 nm Pt–Pd tetrahedrons and cubes. *J. Am. Chem. Soc.* **2011**, *133* (11), 3816–3819.

(19) Feng, J.; Slocik, J. M.; Sarikaya, M.; Naik, R. R.; Farmer, B. L.; Heinz, H. Influence of the shape of nanostructured metal surfaces on adsorption of single peptide molecules in aqueous solution. *Small* **2012**, *8* (7), 1049–59.

(20) Chiu, C.-Y.; Li, Y.; Ruan, L.; Ye, X.; Murray, C.; Huang, Y. Platinum nanocrystals selectively shaped using facet-specific peptide sequences. *Nat. Chem.* **2011**, *3* (5), 393–399.

(21) *Materials Studio*, v 6.0; Accelrys; San Diego, CA, 2012.

(22) Oren, E. E.; Tamerler, C.; Sarikaya, M. Metal recognition of septapeptides via polypod molecular architecture. *Nano Lett.* **2005**, *5* (3), 415–9.

(23) MacKerell, A. D.; Bashford, D.; Bellott, M.; Dunbrack, R. L.; Evanseck, J. D.; Field, M. J.; Fischer, S.; Gao, J.; Guo, H.; Ha, S.; Joseph-McCarthy, D.; Kuchnir, L.; Kucera, K.; Lau, F. T. K.; Mattos, C.; Michnick, S.; Ngo, T.; Nguyen, D. T.; Prodhom, B.; Reiher, W. E.; Roux, B.; Schlenkrich, M.; Smith, J. C.; Stote, R.; Straub, J.; Watanabe, M.; Wiorkiewicz-Kuczera, J.; Yin, D.; Karplus, M. All-atom empirical potential for molecular modeling and dynamics studies of proteins. *J. Phys. Chem. B* **1998**, *102* (18), 3586–3616.

(24) Dauber-Osguthorpe, P.; Roberts, V. A.; Osguthorpe, D. J.; Wolff, J.; Genest, M.; Hagler, A. T. Structure and energetics of ligand binding to proteins: Escherichia coli dihydrofolate reductase-trimethoprim, a drug-receptor system. *Proteins* **1988**, *4* (1), 31–47.

(25) Willett, R. L.; Baldwin, K. W.; West, K. W.; Pfeiffer, L. N. Differential adhesion of amino acids to inorganic surfaces. *Proc. Natl. Acad. Sci. U.S.A.* **2005**, *102* (22), 7817–7822.

(26) Michaelides, A.; Ranea, V. A.; de Andres, P. L.; King, D. A. General model for water monomer adsorption on close-packed transition and noble metal surfaces. *Phys. Rev. Lett.* **2003**, *90*, 21.

(27) Schwierz, N.; Horinek, D.; Netz, R. Anionic and cationic Hofmeister effects on hydrophobic and hydrophilic surfaces. *Langmuir* **2013**, *29* (8), 2602–2614.

(28) Godec, A.; Gaberšček, M.; Jamnik, J.; Janežič, D.; Merzel, F. Ion-size effect within the aqueous solution interface at the Pt(111) surface: molecular dynamics studies. *Phys. Chem. Chem. Phys.* **2010**, *12* (41), 13566–13573.

(29) Lee, K. H.; Ytreberg, F. M. Effect of gold nanoparticle conjugation on peptide dynamics and structure. *Entropy* **2012**, *14* (4), 630–641.

(30) Ruan, L.; Ramezani-Dakhel, H.; Chiu, C. Y.; Zhu, E.; Li, Y.; Heinz, H.; Huang, Y. Tailoring molecular specificity toward a crystal facet: a lesson from biorecognition toward pt{111}. *Nano Lett.* **2013**, *13* (2), 840–6.

(31) Roszak, S.; Balasubramanian, K. Theoretical-study of the interaction of benzene with platinum atom and cation. *Chem. Phys. Lett.* **1995**, *234* (1–3), 101–106.

(32) Schimmel, P. R.; Flory, P. J. Conformational energies and configurational statistics of copolypeptides containing l-proline. *J. Mol. Biol.* **1968**, *34* (1), 105–120.

(33) Zaragoza, I.; Salcedo, R.; Vergara, J. DFT: a dynamic study of the interaction of ethanol and methanol with platinum. *J. Mol. Model.* **2009**, *15* (5), 447–451.

(34) Heinz, H.; Vaia, R. A.; Farmer, B. L.; Naik, R. R. Accurate simulation of surfaces and interfaces of face-centered cubic metals using 12–6 and 9–6 Lennard-Jones potentials. *J. Phys. Chem. C* **2008**, *112* (44), 17281–17290.